

Asymmetric Catalysis

Atroposelective Synthesis of N-Arylated Quinoids by Organocatalytic Tandem N-Arylation/Oxidation

Chang-Qiu Guo⁺, Chuan-Jun Lu⁺, Li-Wen Zhan, Peng Zhang, Qi Xu, Jia Feng, and Ren-Rong Liu*

Abstract: Diarylamines and related scaffolds are ubiquitous atropisomeric chemotypes in biologically active natural products. However, the catalytic asymmetric synthesis of these axially chiral compounds remains largely unexplored. Herein, we report that a BINOL-derived chiral phosphoric acid (CPA) successfully catalyzed the atroposelective coupling of quinone esters and anilines through direct C–N bond formation to afford N-aryl quinone atropisomers with an unprecedented intramolecular N–H–O hydrogen bond within a six-membered ring in good yields and enantioselectivities with the quinone ester as both the electrophile and the oxidant. A gram-scale experiment demonstrated the utility of this synthetic protocol. Moreover, this methodology provides a platform for the synthesis of structurally diverse secondary amine atropisomers by nucleophilic addition.

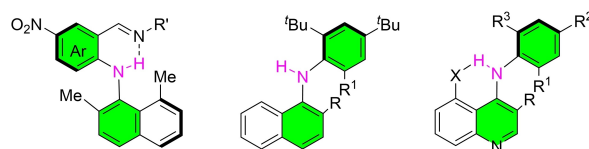
Atropisomerism is a type of axial chirality that originates from the hindered free rotation of a molecule about an axis. Over the past few decades, significant efforts have been devoted to the construction of axially chiral molecules.^[1] Numerous structurally unique atropisomers with axial chirality, such as (hetero)biaryls,^[2] anilides,^[3] and aryl alkenes,^[4] have attracted considerable attention from organic chemists. Diarylamines and related scaffolds are among the most common structural motifs in a myriad of biologically active natural products and pharmaceuticals, such as the FDA-approved drugs bosutinib and binimetinib, and other non-nucleoside reverse transcriptase (NNRT) and vascular endothelial growth factor receptor (VEGFR) inhibitors.^[5] Because of their low rotation barrier, diarylamine atropisomers are configurationally unstable and readily interchangeable. As compared to the synthesis of other stable atropisomers, the introduction of axial chirality into diarylamines and related scaffolds remains challenging.

In 2009, Kawabata resolved a series of diarylamine atropisomers that possessed an internal N–H–N hydrogen

bond by chiral high-performance liquid chromatography (HPLC).^[6] They discovered that the formation of an intramolecular H-bond, leading to a binaphthyl surrogate, was necessary to maintain the stable axial chirality (Scheme 1A). Racemization of diarylamine atropisomers upon heating showed that the energy barrier to racemization was up to 28.2 kcal mol⁻¹. Clayden resolved atropisomeric enantiomers of acyclic diarylamines without intramolecular hydrogen bonding using four *ortho* substituents by chiral HPLC. Moreover, they investigated the racemization of diarylamines by heating and computational studies and deter-

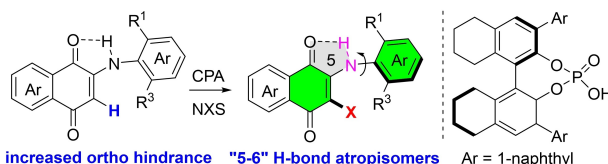
A. Previous reported diarylamine atropisomers (HPLC resolution)

Kawabata's diarylamines Clayden's diarylamines Gustafson's diarylamines

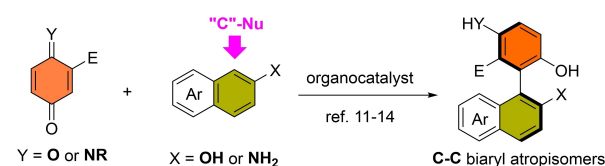


ΔG_{rac} up to 28.2 kcal/mol ΔG_{rac} up to 31.1 kcal/mol ΔG_{rac} up to 36 kcal/mol

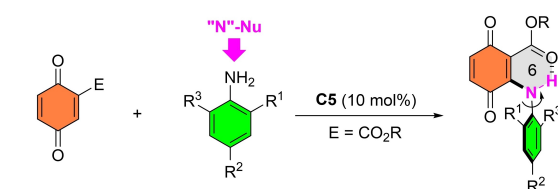
B. The CPA-catalyzed electrophilic halogenation for the synthesis of N-aryl quinones



C. Atroposelective synthesis of C–C atropisomers with quinones and related scaffolds



D. Synthesis of N-aryl quinones by tandem N-arylation/oxidation (this work)



New atropisomeric framework: "6-6" H-bond atropisomers

- Direct C–N bond formation
- Platform for 2° amine atropisomers
- Tandem N-arylation/oxidation
- Up to 84% yield and 99% ee

Scheme 1. Representative atropisomers containing diarylamines and related scaffolds.

[*] C.-Q. Guo,⁺ Dr. C.-J. Lu,⁺ P. Zhang, Q. Xu, Dr. J. Feng, Prof. Dr. R.-R. Liu

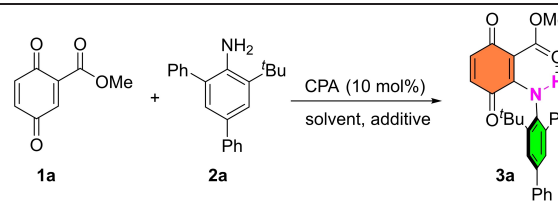
College of Chemistry and Chemical Engineering, Qingdao University
 Ningxia Road 308#, Qingdao 266071 (China)
 E-mail: renrongliu@qdu.edu.cn

[†] These authors contributed equally to this work.

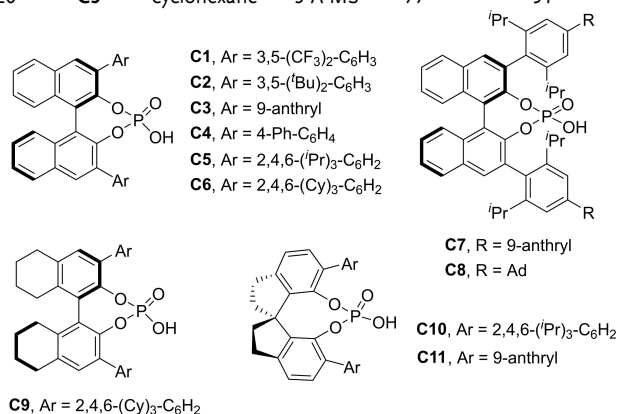
mined the barrier to racemization to be up to 31.1 kcal mol⁻¹.^[7] More recently, Gustafson synthesized highly atropisomerically stable diarylamines with barriers to racemization of 30–36 kcal mol⁻¹ by incorporating increased conjugation into an electron-poor heterocyclic scaffold and introducing intramolecular hydrogen bonding.^[8] However, all three preparation methods for optically active diarylamine atropisomers remain dependent on chiral resolution because the atroposelective construction of axially chiral diarylamines and related scaffolds remains challenging. Gustafson recently reported a chiral-phosphoric-acid-catalyzed enantioselective electrophilic halogenation reaction that afforded a range of stereochemically stable *N*-aryl quinones in good yields and enantioselectivities (Scheme 1 B); this is the first atroposelective synthesis of secondary amine atropisomers in the literature.^[9] Quinones and related scaffolds have long been used as synthetic precursors for chiral compounds.^[10] Recently, Tan,^[11] Kürti,^[12] Bella,^[13] and Miller^[14] have made significant contributions to the synthesis of a variety of non-*C*₂-symmetric axially chiral biaryls with 2-naphthol or 2-naphthylamine as the carbon nucleophile (Scheme 1C). However, nitrogen nucleophiles have not been applied to these asymmetric catalytic reactions thus far. Inspired by these studies and our continuing interest in the field of atropisomeric synthesis,^[15] we report herein the direct C–N bond formation of anilines and quinones for constructing axially chiral *N*-aryl quinones with an unprecedented six-membered intramolecular N–H–O hydrogen bond.^[16] A bifunctional chiral phosphoric acid was used as the catalyst, and the synthesis consisted of tandem conjugated addition, chirality transfer, and oxidation (Scheme 1D).

We initiated our investigation using quinone ester **1a** and aniline **2a** in hexane at room temperature in the presence of the typically used phosphoric acid catalyst (Table 1).^[17] When BINOL-derived CPA **C1** was used as the catalyst, the tandem *N*-arylation/oxidation proceeded smoothly to afford *N*-aryl quinone **3a** in 47% yield, albeit with low enantiocontrol (entry 1). In this reaction, the oxidative capability of excess quinone ester **1a** facilitated the oxidation reaction. Based on this promising result, a series of BINOL-derived CPA catalysts **C2**–**C8** bearing different 3,3'-substituents were screened to improve the enantioselectivity of *N*-aryl quinone **3a** (entries 2–8). In general, phosphoric acid catalysts with bulky substituents at the 3,3'-position afforded good enantiocontrol (entries 5–8). With (*R*)-TRIP **C5** catalyzed the reaction effectively and afforded the highest enantioselectivity (83% ee) among the reactions performed (entry 5). Comparable results were obtained when **C6** bearing the 3,3'-(2,4,6-(Cy)₃-C₆H₂) group was used (entry 6). A bulkier group at the 3,3'-position than 2,4,6-(*i*Pr)₃-C₆H₂ did not further improve the enantioselectivity of **3a** (entries 7–8). When the backbone of CPA was changed from BINOL to H8-BINOL and SPINOL, no further improvement in the enantioselectivity was observed (entries 9–11). The evaluation of different solvents (entries 12–14) showed that cyclohexane afforded a higher enantioselectivity than that obtained by hexane (entry 14 vs. entry 5). Moreover, the additive effect was examined using

Table 1: Optimization of the reaction conditions.^[a]

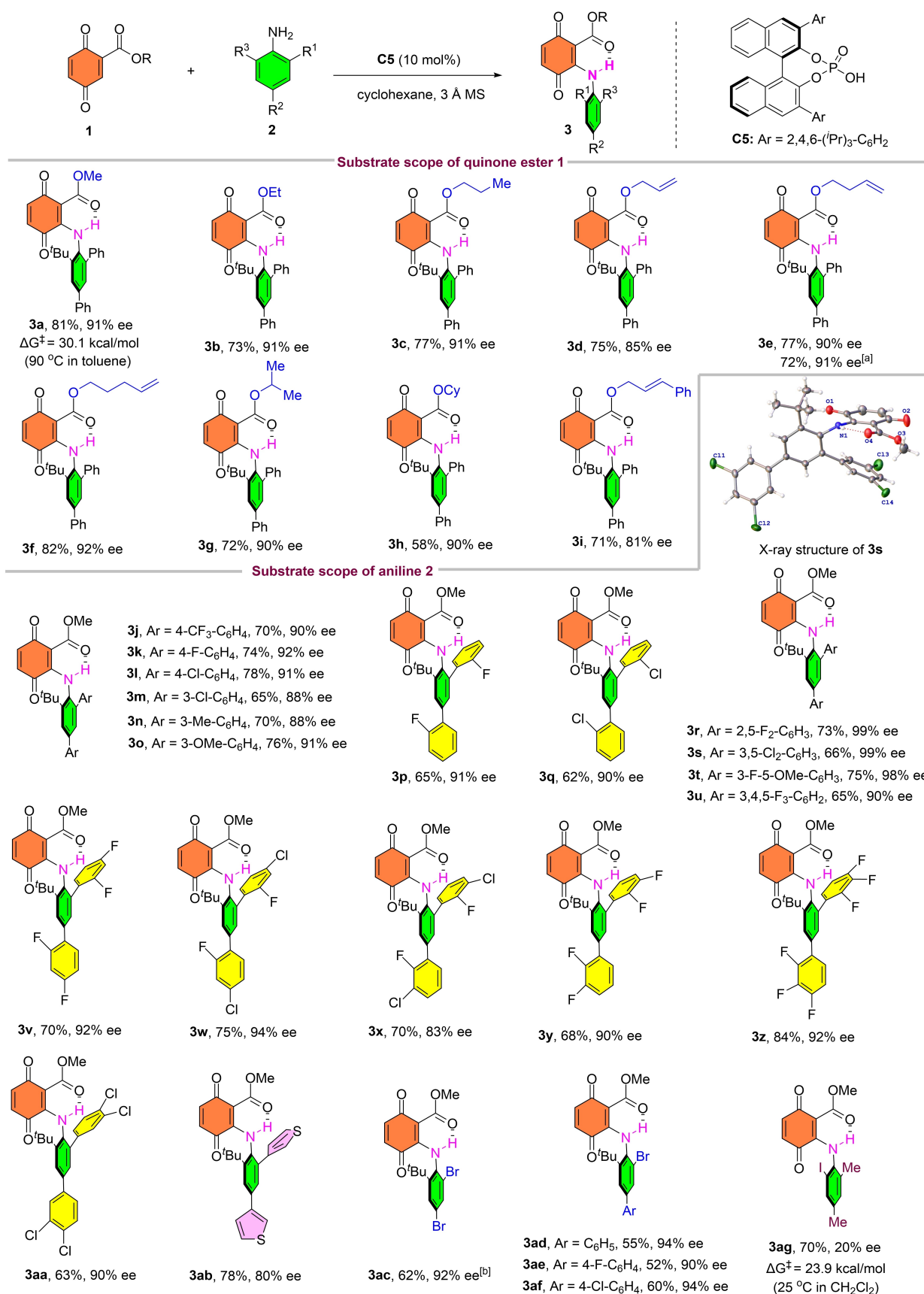


Entry	CPA	Solvent	Additive	Yield [%] ^[b]	ee [%] ^[d]
1	C1	hexane		47	12
2	C2	hexane		40	35
3	C3	hexane		60	61
4	C4	hexane		64	62
5	C5	hexane		72	83
6	C6	hexane		70	80
7	C7	hexane		61	81
8	C8	hexane		70	80
9	C9	hexane		52	50
10	C10	hexane		55	62
11	C11	hexane		57	58
12	C5	CCl ₄		75	77
13	C5	CH ₂ Cl ₂		70	64
14	C5	cyclohexane		75	85
15 ^[d]	C5	cyclohexane	MgSO ₄	62	84
16 ^[e]	C5	cyclohexane	3 Å MS	77	87
17 ^[f]	C5	cyclohexane	4 Å MS	74	85
18 ^[g]	C5	cyclohexane	5 Å MS	77	86
19 ^[h]	C5	cyclohexane	3 Å MS	81	91
20 ^[i]	C5	cyclohexane	3 Å MS	77	91



[a] Reaction conditions: 2-methoxycarbonyl-1,4-benzoquinone (**1a**, 0.22 mmol), 5'-(*tert*-butyl)[1,1':3',1''-terphenyl]-4'-amine (**2a**, 0.10 mmol), and CPA catalyst (10 mol%) in 2.0 mL of solvent at room temperature for 16 h, unless noted otherwise. [b] Isolated yield. [c] Determined by chiral HPLC. [d] MgSO₄ (100 mg) was added. [e] 3 Å MS (100 mg) was added. [f] 4 Å MS (100 mg) was added. [g] 5 Å MS (100 mg) was added. [h] Reaction was performed at 10 °C for 24 h. [i] With **1a** (0.11 mmol), **2a** (0.10 mmol) and DDQ (0.1 mmol). DDQ: 2,3-dichloro-5,6-dicyano-1,4-benzoquinone.

MgSO₄ and different molecular sieves (MS) (entries 15–18). Using 3 Å MS as an additive slightly improved the enantioselectivity to 87% ee and afforded the desired product in 77% yield (entry 16). Lowering the reaction temperature to 10 °C significantly improved the enantioselectivity to 91% ee. Furthermore, with DDQ as an external oxidant, **3a** was achieved in 77% yield with comparable ee (entry 20). Therefore, the optimized conditions were deter-



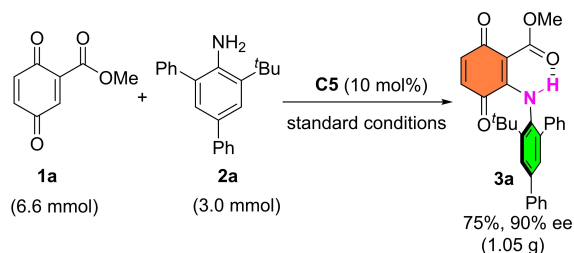
Scheme 2. Reaction conditions: quinone ester 1 (0.22 mmol), aniline 2 (0.1 mmol), CPA catalyst C5 (10 mol%) and 3 Å MS (100 mg) in cyclohexane (2.0 mL) at 10 °C for 24 h, unless noted otherwise. [a] With DDQ (0.10 mmol) as an external oxidant. [b] CCl₄ was used as the solvent instead of cyclohexane.

mined to be: **1a** (0.22 mol), **2a** (0.10 mol), **C5** (10 mol %), and 3 Å MS (100 mg) in 2.0 mL of cyclohexane at 10 °C for 24 h. Then, a preliminary analysis of the stability of the six-membered hydrogen-bonded atropisomer **3a** was conducted. The racemization barrier (ΔG^\ddagger) of **3a** was determined to be 30.1 kcal mol⁻¹ at 90 °C in toluene (see Supporting Information for details)^[18] and is categorized as the class-3 atropisomer based on LaPlante and Edwards's atropisomer stability classification system.^[19]

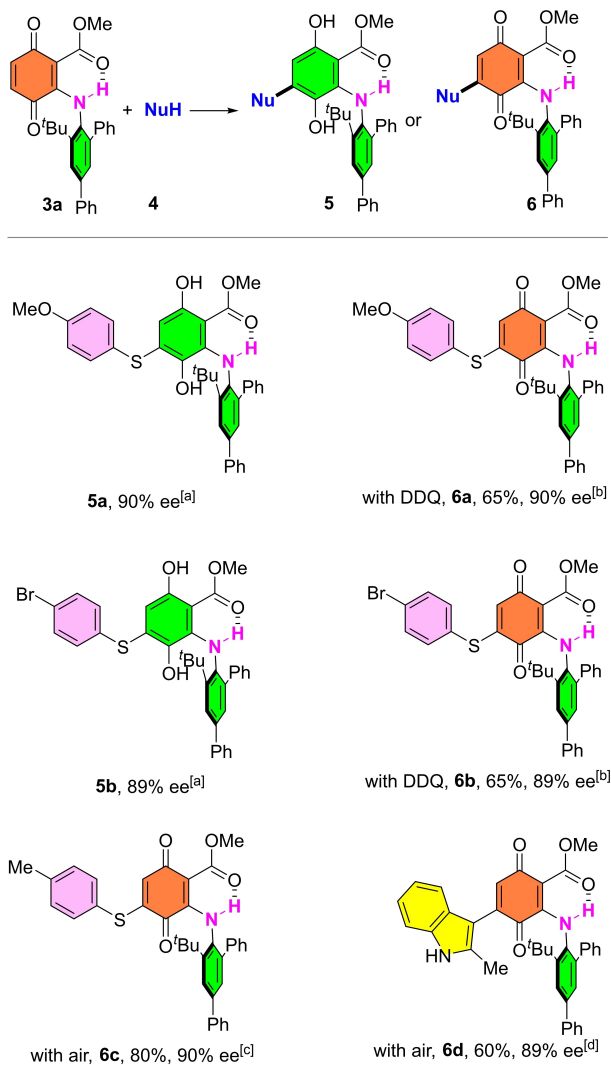
The synthetic merit of this protocol was demonstrated by varying the quinone esters **1** and aniline substrates **2**, and the results are summarized in Scheme 2. Generally, the phosphoric acid catalyzed tandem *N*-arylation/oxidation proceeded smoothly with a variety of quinone esters to provide the corresponding products in 58–82 % yield and 81–92 % ee under mild reaction conditions. Introducing functional groups such as alkenes in the quinone esters (**3d**, **3e**, **3f**, and **3i**) would afford further derivatization. Subsequently, we explored the influence of structural changes in aniline on the yield and enantioselectivity of the *N*-aryl quinone atropisomers. The tandem reaction tolerated diverse aryl substitutions at the 2- and 4-positions of anilines. Aryl groups bearing halogens (**3k**, **3l**, **3m**), CF₃ (**3j**), alkyl (**3n**), and alkoxy (**3o**) on the *para* or *meta* position were well-tolerated, affording the products in 65–78 % yields and 88–92 % ee. The ee values for electron-rich aryl substitutions were higher than those for electron-poor aryl substitutions (**3m** vs **3o**). Aryl groups with *ortho*-substituted groups were also tolerated well to afford the products in good yields (**3p**, **3q**). Moreover, 2,3- (**3x–3y**), 2,4- (**3v–3w**), 2,5- (**3r**), 3,4- (**3aa**), and 3,5- (**3s–3t**) disubstituted as well as 2,3,4- (**3z**) and 3,4,5- (**3u**) trisubstituted aryl groups were also well-tolerated, affording the products in 63–84 % yield and 83–99 % ee. X-ray crystallographic analysis showed that **3s** was the *S* atropisomer.^[20] Moreover, a heteroaromatic-substituted aryl group was incorporated to afford the thiophene derivative **3ab** in 78 % yield and 80 % ee. Aniline with an *ortho*-halogen substituent produced the *N*-aryl quinones **3ac–3af** in good to excellent yields and 90–94 % ee. When an iodo group was substituted in place of the *ortho*-*t*-butyl group, a large decrease in ee (20 %) was observed for the product **3ag**. The racemization barrier of compound **3ag** was measured to be 23.9 kcal mol⁻¹. It is likely due to a low rotational barrier for the atropisomer leading to racemization during the course of the reaction.^[21]

A gram-scale reaction of quinone ester **1a** and aniline **2a** was performed under the standard conditions, which furnished **3a** in 75 % yield and comparable enantioselectivity, demonstrating the scalability of this method (Scheme 3A). The significance of this synthetic protocol was further highlighted by building structurally diverse *N*-aryl quinone atropisomers from this platform molecule **3a** by nucleophilic addition reactions (Scheme 3B). When the nucleophile 4-methoxybenzenethiol **4a** was employed, diarylamine atropisomer **5a** was generated rapidly by Michael addition without any decrease in the ee value. However, rapid oxidation upon air exposure during column chromatography hindered the isolation of **5a**. Therefore, we re-oxidized **5a** with DDQ, thus generating the highly function-

A. Gram-scale reaction of quinone ester **1a** and aniline substrate **2a**



B. Construction of diarylamine and *N*-aryl quinoid atropisomers from **3a**

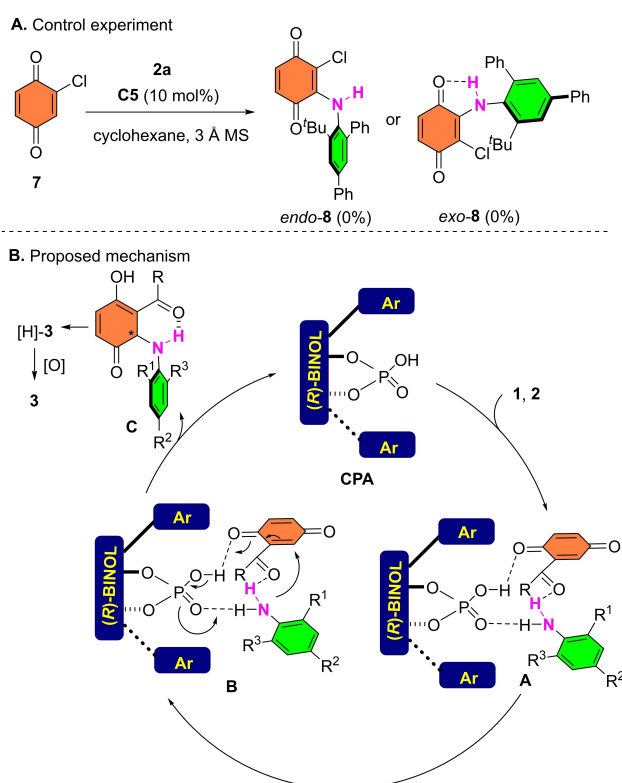


Scheme 3. Reaction conditions: [a] **3a** (0.1 mmol), **4** (0.2 mmol), MeOH/toluene = 1/1 (1.0 mL), under N₂, at 25 °C for 1 h. [b] **3a** (0.1 mmol), **4** (0.2 mmol), MeOH/toluene = 1/1 (1.0 mL), under N₂, at 25 °C for 4 h, then DDQ (0.12 mmol) was added in one portion and stirred for 2 h. [c] **3a** (0.1 mmol), **4c** (0.2 mmol), MeOH/toluene = 1/1 (1.0 mL), under air, at 25 °C for 12 h. [d] **3a** (0.1 mmol), **4d** (0.2 mmol), Sc(OTf)₃ (20 mol %), toluene (1.0 mL), under air, at 25 °C for 12 h.

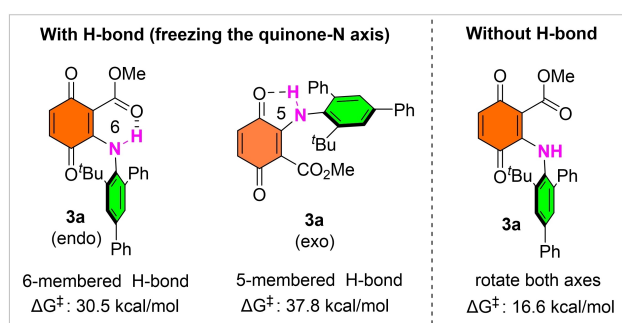
alized *N*-aryl quinone atropisomer **6a** in 65 % yield and 90 % ee. *para*-Bromophenanthiol **4b** and *para*-methyl phenanthiol **4c** also reacted well in this functionalization reaction. Notably, even under air, *N*-aryl quinone atropisomer **6c**

could be obtained in 80 % yield and with 90 % ee. Moreover, the representative C-nucleophile indole reacted smoothly with **3a** catalyzed by Sc(OTf)₃ to furnish the corresponding *N*-aryl quinone atropisomer **6d** in 60 % yield without a significant decrease in the ee value.

Subsequently, preliminary experiments were performed to elucidate the reaction mechanism (Scheme 4A). When chloro-substituted quinone **7** and aniline **2a** were treated under standard conditions, an *N*-arylation/oxidation product *endo*-**8** or *exo*-**8** with a five-membered intramolecular N–H–O hydrogen bonded ring was not produced. This result indicates that carbonyl groups play an important role in the construction of the six-membered hydrogen-bonded ring during the reaction. The possibility that the chloride substrate is less electrophilic than the ester cannot be excluded. Based on these results and previous reports,^[11] a



Scheme 4. Control experiment and proposed catalytic cycle.



Scheme 5. Racemization mechanism of **3a**.

plausible catalytic cycle was proposed (Scheme 4B). Initially, the bifunctional organocatalyst CPA simultaneously activates quinone ester **1** and aniline **2** through multiple H-bonds to form intermediate **A**. This promotes asymmetric conjugate addition to form central chiral intermediate **C** with a six-membered intramolecular N–H–O hydrogen bonded ring via intermediate **B**. Subsequent tautomerization of intermediate **C** results in the transfer of central chirality to axial chirality and affords hydroquinone [H]-**3**. The oxidation of hydroquinone intermediate furnishes the final *N*-aryl quinone atropisomer **3**.

The mechanism of racemization was then explored by computationally evaluating the rotation barriers of **3a** (Scheme 5). When the quinone-N axis is frozen with a six-membered intramolecular N–H–O hydrogen bond, the calculated barrier to rotation ($\Delta G^\ddagger = 30.5 \text{ kcal mol}^{-1}$) agreed with our experimentally determined value ($\Delta G^\ddagger = 30.1 \text{ kcal mol}^{-1}$ in toluene). Whereas the rotation barrier ($\Delta G^\ddagger = 37.8 \text{ kcal mol}^{-1}$) was much higher than the experimental value with a five-membered intramolecular N–H–O hydrogen bond. Moreover, the calculated barrier to rotation was significantly lower than the experimental value via a gearing rotation without the H-bond ($\Delta G^\ddagger = 16.6 \text{ kcal mol}^{-1}$). These studies supported that the racemization could occur through formation of a H-bond with the ester carbonyl group and rotation.

In conclusion, we have developed an efficient enantioselective synthesis of *N*-aryl quinone atropisomers using a chiral phosphoric acid as the catalyst under mild conditions, in a process which occurred by tandem *N*-arylation/oxidation reactions. A broad range of functionalized *N*-aryl quinone atropisomers were conveniently constructed in high yields with excellent enantioselectivities. The utility of the current protocol was highlighted by a successful gram-scale experiment. Furthermore, the obtained *N*-aryl quinone atropisomers serve as platform molecules for the synthesis of structurally diverse secondary amine atropisomers through the nucleophilic addition of thiophenols and indoles and subsequent oxidation.

Acknowledgements

We are grateful for the generous support from the Taishan Scholar Youth Expert Program in Shandong Province (tsqn201909096), National Natural Science Foundation of China (21901236), and the startup fund from Qingdao University. We thank Dr. Yingzi Li for calculating the mechanism of racemization.

Conflict of Interest

The authors declare no conflict of interest.

Data Availability Statement

The data that support the findings of this study are available in the supplementary material of this article.

Keywords: Atropisomerism • C–N Bond Formation • Hydrogen Bonds • Organocatalysis • Quinones

- [1] a) G. Bringmann, T. Gulder, T. A. M. Gulder, M. Breuning, *Chem. Rev.* **2011**, *111*, 563–639; b) J. E. Smyth, N. M. Butler, P. A. Keller, *Nat. Prod. Rep.* **2015**, *32*, 1562–1583; c) S. T. Toenjes, J. L. Gustafson, *Future Med. Chem.* **2018**, *10*, 409–422.
- [2] a) J. Wencel-Delord, A. Panossian, F. R. Leroux, F. Colobert, *Chem. Soc. Rev.* **2015**, *44*, 3418–3430; b) Y. B. Wang, B. Tan, *Acc. Chem. Res.* **2018**, *51*, 534–547; c) A. J. Metrano, S. J. Miller, *Acc. Chem. Res.* **2019**, *52*, 199–215; d) B. Zilate, A. Castrogiovanni, C. Sparr, *ACS Catal.* **2018**, *8*, 2981–2988; e) T. Z. Li, S. J. Liu, W. Tan, F. Shi, *Chem. Eur. J.* **2020**, *26*, 15779–15792; f) Y.-C. Zhang, F. Jiang, F. Shi, *Acc. Chem. Res.* **2020**, *53*, 425–446; g) G. Liao, T. Zhou, Q.-J. Yao, B.-F. Shi, *Chem. Commun.* **2019**, 55, 8514–8523; h) B.-C. Da, S.-H. Xiang, S. Li, B. Tan, *Chin. J. Chem.* **2021**, *39*, 1787–1796; i) C.-X. Liu, W.-W. Zhang, S.-Y. Yin, Q. Gu, S.-L. You, *J. Am. Chem. Soc.* **2021**, *143*, 14025–14040; j) P. Zhang, J. Feng, R.-R. Liu, *Synlett* **2022**, *33*, 1589–1595; k) X. Zhang, K. Zhao, Z. Gu, *Acc. Chem. Res.* **2022**, *55*, 1620–1633.
- [3] a) D. Bonne, J. Rodriguez, *Eur. J. Org. Chem.* **2018**, 2417–2431; b) J. Frey, S. Choppin, F. Colobert, J. Wencel-Delord, *Chimia* **2020**, *74*, 883–889; c) J. Wang, C. Zhao, J. Wang, *ACS Catal.* **2021**, *11*, 12520–12531; d) O. Kitagawa, *Acc. Chem. Res.* **2021**, *54*, 719–730; e) J. Wencel-Delord, F. Colobert, *SynOpen* **2020**, *04*, 107–115; f) G.-J. Mei, W. L. Koay, C.-Y. Guan, Y. Lu, *Chem* **2022**, *8*, 1855–1893; g) Y.-J. Wu, G. Liao, B.-F. Shi, *Green Synth. Catal.* **2022**, *3*, 117–136; h) J. K. Cheng, S. H. Xiang, S. Li, L. Ye, B. Tan, *Chem. Rev.* **2021**, *121*, 4805–4902.
- [4] a) J. Feng, Z. Gu, *SynOpen* **2021**, *5*, 68–85; b) S. Wu, S.-H. Xiang, J. K. Cheng, B. Tan, *Tetrahedron Chem* **2022**, *1*, 100009.
- [5] a) N. M. Levinson, S. G. Boxer, *PLoS One* **2012**, *7*, e29828; b) P. Koelblinger, J. Dornbierer, R. Dummer, *Future Oncol.* **2017**, *13*, 1755; c) Q. Liu, Y. Sabnis, Z. Zhao, T. Zhang, S. J. Buhrlage, L. H. Jones, N. S. Gray, *Chem. Biol.* **2013**, *20*, 146–159; d) S. Han, Y. Sang, Y. Wu, Y. Tao, C. Pannecouque, E. De Clercq, C. Zhuang, F.-E. Chen, *ACS Infect. Dis.* **2020**, *6*, 787–801.
- [6] a) T. Kawabata, C. Jiang, K. Hayashi, K. Tsubaki, T. Yoshimura, S. Majumdar, T. Sasamori, N. Tokitoh, *J. Am. Chem. Soc.* **2009**, *131*, 54–55; b) K. Hayashi, N. Matubayasi, C. Jiang, T. Yoshimura, S. Majumdar, T. Sasamori, N. Tokitoh, T. Kawabata, *J. Org. Chem.* **2010**, *75*, 5031–5036.
- [7] a) R. Costil, H. J. A. Dale, N. Fey, G. Whitcombe, J. V. Matlock, J. Clayden, *Angew. Chem. Int. Ed.* **2017**, *56*, 12533–12537; *Angew. Chem.* **2017**, *129*, 12707–12711; b) R. Costil, A. J. Sterling, F. Duarte, J. Clayden, *Angew. Chem. Int. Ed.* **2020**, *59*, 18670–18678; *Angew. Chem.* **2020**, *132*, 18829–18837.
- [8] S. D. Vaidya, B. S. Heydari, S. T. Toenjes, J. L. Gustafson, *J. Org. Chem.* **2022**, *87*, 6760–6768.
- [9] a) S. D. Vaidya, S. T. Toenjes, N. Yamamoto, S. M. Maddox, J. L. Gustafson, *J. Am. Chem. Soc.* **2020**, *142*, 2198–2203; For an electrophilic sulfenylation reaction, see: b) D. Zhu, L. Yu, H.-Y. Luo, X.-S. Xue, Z.-M. Chen, *Angew. Chem. Int. Ed.* **2022**, *61*, e202211782; *Angew. Chem.* **2022**, *134*, e202211782.
- [10] a) D. A. Evans, J. Wu, *J. Am. Chem. Soc.* **2003**, *125*, 10162–10163; b) J. Alemán, B. Richter, K. A. Jørgensen, *Angew. Chem. Int. Ed.* **2007**, *46*, 5515–5519; *Angew. Chem.* **2007**, *119*, 5611–5615; c) J. Alemán, S. Cabrera, E. Maerten, J. Overgaard, K. A. Jørgensen, *Angew. Chem. Int. Ed.* **2007**, *46*, 5520–5523; *Angew. Chem.* **2007**, *119*, 5616–5619; d) L. Liao, C. Shu, M. Zhang, Y. Liao, X. Hu, Y. Zhang, Z. Wu, W. Yuan, X. Zhang, *Angew. Chem. Int. Ed.* **2014**, *53*, 10471–10475; *Angew. Chem.* **2014**, *126*, 10639–10643; e) Y.-C. Zhang, J.-J. Zhao, F. Jiang, S.-B. Sun, F. Shi, *Angew. Chem. Int. Ed.* **2014**, *53*, 13912–13915; *Angew. Chem.* **2014**, *126*, 14132–14135; f) C. Xu, H. Zheng, B. Hu, X. Liu, L. Lin, X. Feng, *Chem. Commun.* **2017**, *53*, 9741–9744; g) Q.-J. Liu, J. Zhu, X.-Y. Song, L. Wang, S. R. Wang, Y. Tang, *Angew. Chem. Int. Ed.* **2018**, *57*, 3810–3814; *Angew. Chem.* **2018**, *130*, 3872–3876; h) W. Luo, Z. Sun, E. H. N. Ferno, V. N. Nesterov, T. R. Cundari, H. Wang, *Chem. Sci.* **2020**, *11*, 9386–9394; i) C.-C. Xi, X.-J. Zhao, J.-M. Tian, Z.-M. Chen, K. Zhang, F.-M. Zhang, Y.-Q. Tu, J.-W. Dong, *Org. Lett.* **2020**, *22*, 4995–5000; j) T. Hashimoto, H. Nakatsu, Y. Takiguchi, K. Maruoka, *J. Am. Chem. Soc.* **2013**, *135*, 16010–16013.
- [11] a) Y.-H. Chen, D.-J. Cheng, J. Zhang, Y. Wang, X.-Y. Liu, B. Tan, *J. Am. Chem. Soc.* **2015**, *137*, 15062–15065; b) Y.-H. Chen, L.-W. Qi, F. Fang, B. Tan, *Angew. Chem. Int. Ed.* **2017**, *56*, 16308–16312; *Angew. Chem.* **2017**, *129*, 16526–16530; c) S. Zhu, Y.-H. Chen, Y.-B. Wang, P. Yu, S.-Y. Li, S.-H. Xiang, J.-Q. Wang, J. Xiao, B. Tan, *Nat. Commun.* **2019**, *10*, 4268; d) Y.-H. Chen, H.-H. Li, X. Zhang, S.-H. Xiang, S. Li, B. Tan, *Angew. Chem. Int. Ed.* **2020**, *59*, 11374–11378; *Angew. Chem.* **2020**, *132*, 11470–11474.
- [12] a) H. Gao, Q.-L. Xu, C. Keene, M. Yousufuddin, D. H. Ess, L. Kürti, *Angew. Chem. Int. Ed.* **2016**, *55*, 566–571; *Angew. Chem.* **2016**, *128*, 576–581; b) J.-Z. Wang, J. Zhou, C. Xu, H. Sun, L. Kürti, Q.-L. Xu, *J. Am. Chem. Soc.* **2016**, *138*, 5202–5205.
- [13] M. Moliterno, R. Cari, A. Puglisi, A. Antenucci, C. Sperandio, E. Moretti, A. Di Sabato, R. Salvia, M. Bella, *Angew. Chem. Int. Ed.* **2016**, *55*, 6525–6529; *Angew. Chem.* **2016**, *128*, 6635–6639.
- [14] G. Coombs, M. H. Sak, S. J. Miller, *Angew. Chem. Int. Ed.* **2020**, *59*, 2875–2880; *Angew. Chem.* **2020**, *132*, 2897–2902.
- [15] a) X.-M. Wang, P. Zhang, Q. Xu, C.-Q. Guo, D.-B. Zhang, C.-J. Lu, R.-R. Liu, *J. Am. Chem. Soc.* **2021**, *143*, 15005–15010; b) P. Zhang, X.-M. Wang, Q. Xu, C.-Q. Guo, P. Wang, C.-J. Lu, R.-R. Liu, *Angew. Chem. Int. Ed.* **2021**, *60*, 21718–21722; *Angew. Chem.* **2021**, *133*, 21886–21890; c) Q. Xu, H. Zhang, F.-B. Ge, X.-M. Wang, P. Zhang, C.-J. Lu, R.-R. Liu, *Org. Lett.* **2022**, *24*, 3138–3143.
- [16] For asymmetric synthesis of atropisomeric derivatives via direct formation of C–N bonds, see: a) O. Kitagawa, M. Takahashi, M. Yoshikawa, T. Taguchi, *J. Am. Chem. Soc.* **2005**, *127*, 3676–3677; b) S. Brandes, M. Bella, A. Kjaersgaard, K. A. Jørgensen, *Angew. Chem. Int. Ed.* **2006**, *45*, 1147–1151; *Angew. Chem.* **2006**, *118*, 1165–1169; c) S. Shirakawa, K. Liu, K. Maruoka, *J. Am. Chem. Soc.* **2012**, *134*, 916–919; d) S.-L. Li, C. Yang, Q. Wu, H.-L. Zheng, X. Li, J.-P. Cheng, *J. Am. Chem. Soc.* **2018**, *140*, 12836–12843; e) L.-W. Qi, J.-H. Mao, J. Zhang, B. Tan, *Nat. Chem.* **2018**, *10*, 58–64; f) J. Rae, J. Frey, S. Jerhaoui, S. Choppin, J. Wencel-Delord, F. Colobert, *ACS Catal.* **2018**, *8*, 2805–2809; g) H.-Y. Bai, F.-X. Tan, T.-Q. Liu, G.-D. Zhu, J.-M. Tian, T.-M. Ding, Z.-M. Chen, S.-Y. Zhang, *Nat. Commun.* **2019**, *10*, 3063; h) W. Xia, Q.-J. An, S.-H. Xiang, S. Li, Y.-B. Wang, B. Tan, *Angew. Chem. Int. Ed.* **2020**, *59*, 6775–6779; *Angew. Chem.* **2020**, *132*, 6841–6845; i) J. Frey, A. Malekafzali, I. Delso, S. Choppin, F. Colobert, J. Wencel-Delord, *Angew. Chem. Int. Ed.* **2020**, *59*, 8844–8848; *Angew. Chem.* **2020**, *132*, 8929–8933; j) V. Thönnißen, F. W. Patureau, *Chem. Eur. J.* **2021**, *27*, 7189–7192; k) K. Zhao, L. Duan, S. Xu, J. Jiang, Y. Fu, Z. Gu, *Chem* **2018**, *4*, 599–612; l) X. Zhang, K. Zhao, N. Li, J. Yu, L.-Z. Gong, Z. Gu, *Angew. Chem. Int. Ed.* **2020**, *59*, 19899–19904; *Angew. Chem.* **2020**, *132*, 20071–20076.

- [17] a) T. Akiyama, *Chem. Rev.* **2007**, *107*, 5744–5758; b) M. Terada, *Chem. Commun.* **2008**, 4097–4112; c) D. Parmar, E. Sugiono, S. Raja, M. Rueping, *Chem. Rev.* **2014**, *114*, 9047–9153.
- [18] The H-bond properties of the solvents have some effect on the rotation barriers. Racemization barrier of **3a** was measured to be 28.4 kcal mol⁻¹ at 70 °C in ⁱPrOH and 28.8 kcal mol⁻¹ at 70 °C in THF. Moreover, acidic conditions had slight influence on the stereochemical stability. Racemization barrier of **3a** was measured to be 27.9 kcal mol⁻¹ in a mixture of EtOH and 0.5 M HCl (V_{EtOH}:V_{HCl}=4:1).
- [19] S. R. LaPlante, L. D. D. D. Fader, K. R. Fandrick, D. R. Fandrick, O. Hucke, R. Kemper, S. P. F. Miller, P. J. Edwards, *J. Med. Chem.* **2011**, *54*, 7005–7022.
- [20] Deposition number 2201453 contain the supplementary crystallographic data for this paper. These data are provided free of charge by the joint Cambridge Crystallographic Data Centre and Fachinformationszentrum Karlsruhe Access Structures service.
- [21] Aniline possessed an isopropyl at the 6-position was also evaluated, resulted the product **3ah** in 11 % ee after 5 h at room temperature. Racemization barrier of the isopropyl substituted product was measured to be 23.4 kcal mol⁻¹.

Manuscript received: August 30, 2022

Accepted manuscript online: October 11, 2022

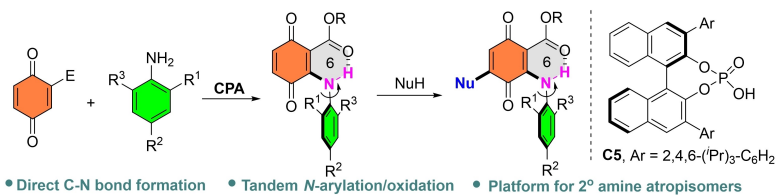
Version of record online: ■■, ■■

Communications

Asymmetric Catalysis

C.-Q. Guo, C.-J. Lu, L.-W. Zhan, P. Zhang,
Q. Xu, J. Feng, R.-R. Liu* — e202212846

Atroposelective Synthesis of N-Arylated
Quinoids by Organocatalytic Tandem N-
Arylation/Oxidation



A chiral-phosphoric-acid-catalyzed process was developed for the asymmetric synthesis of *N*-aryl quinoid atropisomers through direct C–N bond formation. In this way, a broad range of functionalized

N-aryl quinone atropisomers containing an unprecedented intramolecular N–H–O hydrogen bond within a six-membered ring were constructed in high yields with excellent enantioselectivity.